

OPERATING LIQUID METALJET X-RAY SOURCES FOR MATERIALS RESEARCH

Mirko Boin, Roland Mainz, Manuela Klaus, Daniel Apel, Paul H. Kamm, Robert C. Wimpory,
Francisco García-Moreno, Guido Wagener, Christoph Genzel,
Helmholtz-Zentrum Berlin für Materialien und Energie GmbH, Berlin, Germany

Abstract

Even on the 100th anniversary of the death of Wilhelm Conrad Röntgen the demand for applications of his discovery of X-rays is not diminishing. On the contrary, both academic and industrial research and development need X-ray generating devices with ever-improving properties to meet the current challenges of science and technology. For this reason, the development of next-generation synchrotrons is being driven forward and made available to users worldwide. Nevertheless, the availability of synchrotron beamtime will always remain limited, even with the most brilliant sources for ultra-fast and high-throughput experiments. That is why the operation of and research with decentralized laboratory equipment becomes just as important. In this context, Helmholtz-Zentrum Berlin (HZB) has commissioned Excillum's MetalJet X-ray devices providing photon energies in the hard X-ray regime. Technical specifications of these sources, the HZB diffractometer lab installations and selected examples are shown. A comparison to synchrotron measurements is made to benchmark the performance of the available setups.

INTRODUCTION

Non-destructive testing methods utilizing conventional laboratory (desktop) X-ray sources have become a successful tool for more and more academic and industrial research purposes, such that their physical limits, for example according to the material's penetration depths, have been extended using high-energy synchrotron photons. Furthermore, high-brilliance synchrotron photons have made fast in-situ and in-operando experiments possible.

However, the increasing demand for measurement time at such facilities contrasts with their availability – the beamtime at synchrotron sources is very limited. Moreover, as a rule, the access to the beamlines cannot be obtained promptly. Waiting times of half a year or longer are quite common in this field. Synchrotron beamlines are usually overbooked many times. Hence, it seems sensible and necessary in several ways to use suitable laboratory X-ray sources as well. With their help, numerous questions can be answered which do not necessarily require the use of expensive and in their availability mostly very limited large-scale facilities.

It is the motivation of this work to address the lack of beamtime with the development of tailored measurement and evaluation methods including the implementation of appropriate experimental hardware using laboratory X-ray sources. Here, novel X-ray sources are presented that help to transport a number of applications from the synchrotron

to decentralized laboratories and thus make the analysis of microstructural properties available to a larger community.

LIQUID METALJET X-RAY SOURCES

Inside laboratory and desktop X-ray devices electrons are extracted from a cathode and accelerated within an electric field into the direction of an anode, where their deceleration leads to an energy conversion into heat and X-rays. In general, the X-ray power of all electron-impact X-ray sources is limited by the thermal power loading of the anode. In solid-anode technology, the surface temperature of the anode must be cooled down and stay well below its melting point to avoid damage. Consequently, the yield in terms of photon flux of conventional fixed-anode X-ray tubes is rather low compared to synchrotron radiation. Although the X-ray output can be increased significantly with the use of rotating-anode tubes, the melting limitation of the solid anode material remains.

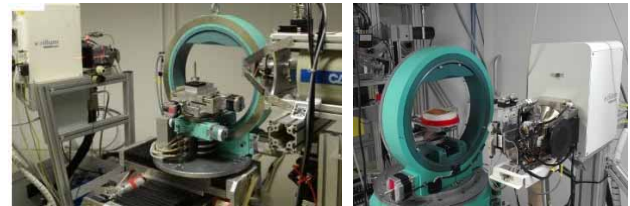


Figure 1: Photographs of the LIMAX-70 (left) and LIMAX-160 (right) laboratories.

In contrast, a liquid metal anode changes this condition since the limitation to maintain the target at well below the melting point is inexistent – the material is already molten. This approach is implemented by the MetalJet products available from the Swedish company Excillum. Two of their MetalJet D2 X-ray sources have been installed at HZB to equip a suite of the so-called LIMAX laboratories (see Fig. 1) for microstructural, residual stress and imaging characterizations. These sources continuously supply fresh target material. The liquid anode, composed of a Ga-In alloy liquid already at room temperature, is provided via a closed high-pressure circuit at 190 bars. A very fine liquid metal jet of a diameter of about 180 μm is formed with the help of a nozzle. The electrons are released by a LaB₆ cathode and accelerated into the direction of the liquid anode under a voltage of 70 kV and 160 kV respectively. With the help of focusing optics a very well-defined electron spot of down to 5 $\mu\text{m} \times 5 \mu\text{m}$ is created at the edge of the metal jet. The X-ray spectrum emitted consists of a broad range of Bremsstrahlung (the white beam) up to 70 keV and 160 keV respectively, depending on the excitation voltage. In addition, and due to the extremely high-power loading,

two very intense K_{α} -emission lines occur at $E = 9.2$ keV for Ga and $E = 24.2$ keV for In, depending on the alloy composition (Fig. 2).

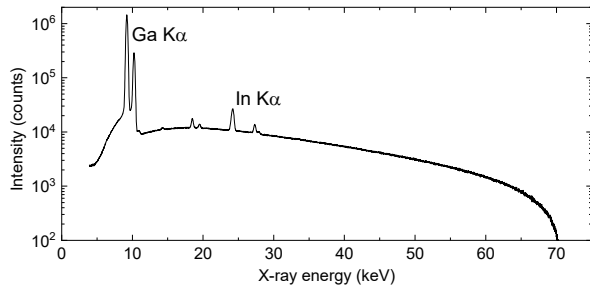


Figure 2: X-ray emission spectrum of the MetalJet D2 measured with LIMAX-70.

Utilizing the so-called Ex-Alloy-I1 target alloy (Ga: 68 wt %; In: 22 wt %; Sn: 10 wt %) the absolute photon fluxes per solid angle have been verified by photon scattering for Ga K_{α} and In K_{α} to be $6.0(5) \times 10^{12} \text{ s}^{-1} \text{ sr}^{-1}$ and $3.8(4) \times 10^{11} \text{ s}^{-1} \text{ sr}^{-1}$, respectively [1] at 200 W emission power and 70 kV acceleration voltage. This agrees very well with the specifications given by Excillum.

The output X-ray windows of the MetalJet devices provide a 10° open cone beam. To shape the beam for diffraction experiments, for example, one obvious way is to cut out the size of your gauge volume with the help of a slit system, collimators and Soller slits. However, to make the most use of the incident intensity, third-party primary optics are available instead. Polycapillary optics are used to guide a large fraction of the emitted photons up to about 40 keV onto the sample by total external reflection from the walls of the thin glass tubes. Higher energies are not guided by such capillary optics such that their detected intensities are significantly lower. To provide monochromatic X-rays so-called Montel-optics are used to select very precisely the Ga K_{α} line, e.g. for angle-dispersive diffraction measurements. Both can be tailored to the needs of a specific experiment setup, i.e. their focus lengths can be either a few centimeters or some meters, for example. At both sources, LIMAX-70 and LIMAX-160, the primary optics – either polycapillary or Montel type – can be aligned by a 6-axis PI H811.I2 hexapod in all directions and orientations to meet the optimum beam conditions, e.g. the maximum intensity.

The LIMAX-70 is equipped with a diffractometer consisting of two Huber 480 goniometer circles, each with a diameter of 800 mm, to realize angle-dispersive diffraction and the rotation of a sample setup respectively. For sample manipulation a large x-y-z stage with a translation range of 250 mm in each direction also allows for heavier setups, such as a stress rig, furnaces or a Huber 512 Euler cradle, for example. In a similar manner, the LIMAX-160 laboratory is modular to change between an Euler cradle based diffractometer setup with integrated x-y-z translation table and other stages, such as a deposition chamber, furnaces and stress-rigs.

A set of detectors with a large range of specifications provide the opportunity for a number of diffraction, radiographic and tomographic experiments. A Dectris Pilatus3 S IM with an X-ray detection area of $169 \times 179 \text{ mm}^2$ divided into 981×1043 pixels, consisting of 10 Si sensor modules each with a size of $83.8 \times 33.5 \text{ mm}^2$ and $1000 \mu\text{m}$ thickness, is available for angle-dispersive X-ray diffraction. Complementary, two energy-resolving LN2-cooled Canberra Ge detectors with a sensor size of $10 \times 10 \text{ mm}^2$ are available for energy-dispersive diffraction measurements. A PCO 1200 hs CMOS camera with a 1280×1024 pixel resolution and short exposures times is used with scintillators to convert X-rays into visible light. Additionally, an Advacam WidePIX detector with a CdTe sensor of $70 \text{ mm} \times 28 \text{ mm}$ and an Advacam MiniPIX detector with a Si Sensor of $14 \times 14 \text{ mm}^2$ – both with a pixel size of $55 \times 55 \mu\text{m}^2$, as well as a Hamamatsu flat panel detector with a $120 \times 120 \text{ mm}^2$ scintillator plate and $50 \times 50 \mu\text{m}^2$ pixel size – are available for imaging experiments. A summary of the setup specifications and available instrument options is given in Table 1. Both laboratories are available for external and in-house users as well as for industrial applications.

Table 1: MetalJet Experimental Setups At HZB

	LIMAX-70	LIMAX-160
Anode alloy	Ga-rich alloy G1	In-enriched alloy I1
Excitation voltage	max. 70 keV	max. 160 keV
X-ray optic options	slits, collimators, capillary optics, Montel optics	
Sample stage	Huber-480 2-circle goniometer of 800 mm diameter with x-y-z stage and optional Euler cradle	Huber-440 goniometer of 500 mm diameter with optional Euler cradle
Sample environment options	(Cryo-)Furnace Load frame PVD chamber Extra rotation stage	
Detector options	Imaging PCO camera WidePIX + MiniPIX detectors Dectris Pilatus IM Hamamatsu flat panel Canberra Ge-detectors	

APPLICATIONS

Taking advantage of the unique features of the X-ray spectrum emitted by the liquid metal jet source, i.e. the characteristic K_{α} -emission lines of Ga and In, as well as the white beam, allows for a multitude of applications and different types of measurements, such as angle- and energy-dispersive diffraction and transmission imaging, for instance.

Energy-Dispersive X-ray Stress Analysis (ED-XSA)

The basic principles of X-ray residual stress analysis rely on the correlation between lattice strain measured in any direction with respect to the sample coordinate system and the components of the stress tensor which is given by the fundamental equation for stress analysis using diffraction methods [2] and the so-called $\sin^2\psi$ method [3]. For the analysis of residual stress depth gradients an extension, taking the exponential attenuation of the X-ray intensity by the investigated material into account, is available [4, 5] and the application to the energy-dispersive case of diffraction has been implemented and used at synchrotron beamlines, such as EDDI@BESSY-II [6, 7], taking advantage of the available white and hard X-ray beam spectrum. The same practice is transferred to the LIMAX labs to make it available to a broader community without the restrictions of the limited access to a synchrotron beamline.

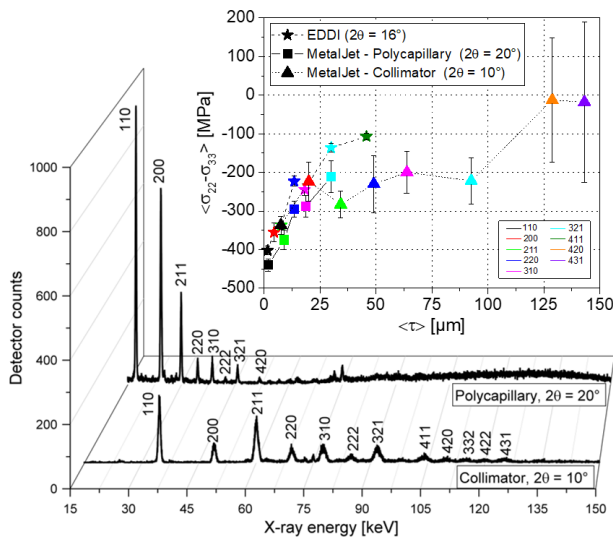


Figure 3: Diffractograms (bottom), measured with the Canberra Ge detector, of a ground steel sample measured at LIMAX-160 with two different settings – and the corresponding residual stress evaluation (top) in comparison to synchrotron results with significantly smaller error bars.

Here, the measurement of a ground C-80 steel sample at the LIMAX-160 source is shown and compared with synchrotron results. The sample surface was measured under two settings with the LIMAX-160 – with polycapillary optics (scattering angle of $2\theta = 20^\circ$) as well as with collimator optics and a scattering angle of $2\theta = 10^\circ$. The measured lattice plane reflections in the diffractograms in Fig. 3 (bottom) are indicated with the hkl Miller indices. The position of the diffraction lines depends on the choice of the selected, but fixed, scattering angle 2θ – with smaller 2θ leading to a broader distribution in the detected energy spectrum. The diffractograms as well as the residual stress depth profiles obtained with the two optics clearly reveal their advantages and drawbacks. The polycapillary lens provides sharp and intense diffraction lines within rather short measuring times up to about 40 keV. Then the glass becomes transparent losing the effect of total reflection.

The collimator, on the other hand, also guides the high energy photons without attenuation, resulting in evaluable diffraction lines up to about 125 keV, which allows to extend the information depth of the residual stress profiles considerably. However, due to the comparably low photon flux (no collimation effect) the counting times per spectrum are very long. The results achieved in both configurations are in good agreement with those obtained before at the EDDI synchrotron beamline.

ED-XSA in Complex Geometries

Nevertheless, the extreme high photon flux and brilliance of modern synchrotron beamlines provides further advantages. Diffraction measurements are possible with even very small gauge volumes and – considering the above-described energy-dispersive method – allow for residual stress experiments on surfaces difficult to access, e.g. on the inside of boreholes in complex-shaped industrial components. Such measurements are not feasible with conventional laboratory X-ray equipment, since the reduction of the X-ray spot size on the sample leads to a very small signal-to-background ratio difficult to analyze.

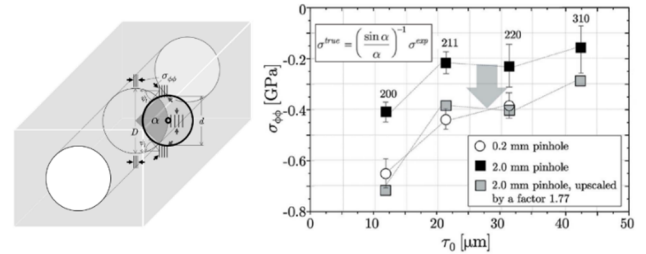


Figure 4: Influence of the X-ray beam size on curved surface (left) on the magnitude of a measured residual stress gradient (right) as taken from [8].

For example, the non-destructive access of the tangential stress component on the inside of a borehole with a large L/D ratio (length-over-diameter) is only feasible with the energy-dispersive diffraction method under small scattering angles, which must be chosen small enough to ‘thread-through’ the incident and diffracted X-ray beam during a $\sin^2\psi$ -scan.

Despite the higher flux of a MetalJet D2, as compared to conventional X-ray sources, a reduction of the beam size is still at the costs of the signal to be evaluated for residual stress depth gradients in the frame of such applications. In the below example the LIMAX-160 was used to measure the tangential stresses at the inner wall of a borehole with a diameter of 2 mm and 10 mm length. For the comparison of two different measurements polycapillary optics were utilized in combination with a 2 mm and a 0.2 mm pinhole. Counting times of 300 s per orientation were used for the larger pinhole and 3600 s for the small pinhole. On the secondary side an equatorial Soller slit with of $\delta = 0.15^\circ$ was installed in front of the detector for both setups. The resulting beam sizes on the inner borehole surface are sketched in Fig. 4 (left). Both beam diameters, as defined by the pinholes, are drawn as bold circles on the inner wall of the borehole.

The influence of the beam diameter on the residual stress evaluation under the effect of such a curved surface is discussed in detail in [8]. It leads to a systematic scaling of the evaluated stress gradient towards lower absolute stresses. The authors have further developed a correction method by putting the geometrical constraints of the borehole and beam diameters into the equations for strain and stress evaluation. In the example in Fig. 4 (right) a correction factor of 1.77 was derived for the measurement with the 2 mm pinhole. Its application onto the evaluated stress gradient finally leads to a perfect match of the evaluated stress curve measured with the 0.2 mm pinhole and to earlier measurements at the synchrotron beamline.

Phase Transitions in Photovoltaic Materials

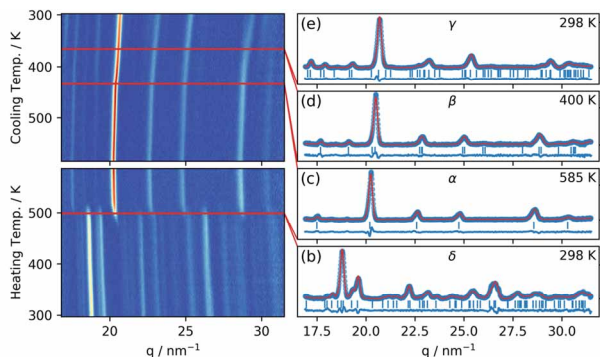


Figure 5: Integrated diffraction pattern measured with the Pilatus detector as a function of temperature for $\text{CsPb}(\text{Br}_x\text{I}_{1-x})_3$ with $x = 0.23$ taken from [9].

The high X-ray flux of the MetalJet sources further enables high-throughput in-situ experiments for the investigation of phase transitions, for example in photovoltaic materials. In this example Grazing-Incidence Wide-Angle X-ray Scattering (GIWAXS) measurements have been conducted to resolve all transition temperatures for a phase diagram from 300 K to 585 K of $\text{CsPb}(\text{Br}_x\text{I}_{1-x})_3$ with a composition range of $0 \leq x \leq 0.68$ in a single heating process [9]. $\text{CsPb}(\text{Br}_x\text{I}_{1-x})_3$ is utilized as a so-called perovskite solar cell material with a beneficial microstructure for high solar energy conversion efficiencies. The MetalJet source was used at 70 kV with an angle-dispersive diffraction setup, polycapillary optics, a 2D detector and a heating stage. The setup allows for fast acquisition of the samples' diffraction patterns on the detector during thermal annealing during formation of the perovskite structure. Preliminary studies have shown that Bromine helps to stabilize a metastable gamma phase structure at room temperature, but the necessary phase diagrams were unexplored before. The measurements with the MetalJet source helped to identify the transition temperatures for all phases. Fig. 5 shows the integrated GIWAXS patterns as a function of temperature during heating up and cooling down. As a result, the transition temperatures decrease with an increasing Bromium content and are in accordance with theoretical calculations.

These findings and experimental confirmations help in the design and the processing of solar cell materials, and

this example has demonstrated, that fast phase diagram studies are feasible with a lab-based setup.

White-beam Imaging

Driven by X-ray tomography, time-resolved tomography, activities at the BESSY II and SLS synchrotron sources [10-12] and the high-flux potential of the Excillum sources, the MetalJet devices and the experimental equipment brings further X-ray imaging opportunities to the user community. The radiographic measurements are conducted with the original cone beam geometry provided by the sources and without primary beam optics.

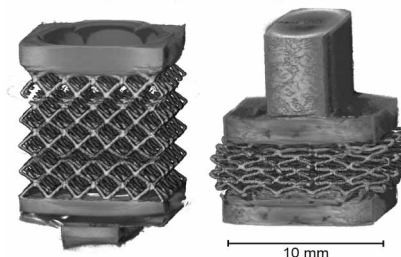


Figure 6: A tomographic reconstruction of an additive-manufactured steel sample.

The photon energies of up to 160 keV allow for the investigation of thicker components and denser materials. The use of the full white beam spectrum gives rise to fast measurements with short acquisition times. Fig. 6, for example, shows the tomographic reconstruction of an additive-manufactured test specimen made of steel in the original and in a compressed state.

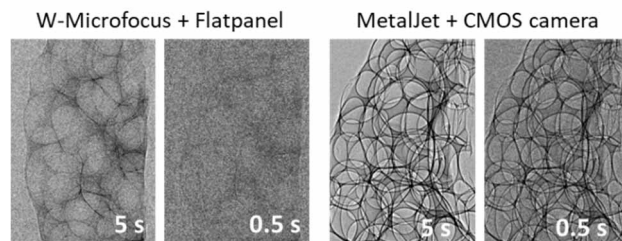


Figure 7: Radiographic images of soft matter foams [13] with different contrast and exposure times measured with a conventional tungsten microfocus tube and a flat panel detector (left) as well as with a MetalJet at 70 kV and the CMOS camera (right).

Depending on the right choice of the available detectors fast measurements of soft matter materials are also feasible within short time ranges – especially in the energy regime of the very intense Ga-K α emission line. The detectors' energy sensitivity varies with their sensor material and leads to different image contrasts [13] such as shown in Fig. 7.

FURTHER DEVELOPMENTS & UPGRADE ACTIVITIES

The above-mentioned applications and methods are constantly being advanced. For the imaging option a new Photonics camera with 4.5 μm pixel size and a 15 μm -thick scintillator has been purchased and will be tested with the

Content from this work may be used under the terms of the CC-BY-4.0 licence © 2023. Any distribution of this work must maintain attribution to the author(s), title of the work, publisher, and DOI

aim to achieve higher spatial resolution for imaging experiments.

A setup for parallel white beam X-ray diffraction and imaging experiments has been realized at the BESSY II synchrotron beamline EDDI [14]. The potential of the MetalJet sources and the available equipment at HZB are currently aiming at a similar approach to make such a method available in decentralized labs.

HZB has further invested in Excillum's latest development – the MetalJet E1+. The new X-ray source uses the same technique of a liquid anode material, but with a total power of 1000 W. The source will extend the HZB activities and the throughput of applications.

CONCLUSION

The MetalJet sources and the HZB equipment described herein demonstrate a wide range of applications to be investigated with hard X-rays by academic users as well as for industrial research in the field of material science. Measurements of energy-resolved residual stress depth-gradients are feasible within complex geometry such as components with boreholes and with information depth comparable to experiments at synchrotron beamlines. Likewise, long-term experiments can be conducted without the restriction of limited beamtime. The high X-ray flux in combination with appropriate measurement and detection methods allows for in-situ investigation which have had been performed earlier at synchrotrons.

The installation, operation, and maintenance of the MetalJet sources are accompanied by higher complexity as compared to conventional X-ray tubes. The need for a 24/7 setup constantly providing high-flux X-rays over a long period requires careful handling of the devices and planning of service intervals. The new equipment at HZB is available to external user and will further bridge the gap between high-flux and high-energy synchrotron photons and conventional desktop-like low-flux X-ray tubes.

REFERENCES

- [1] M. Wansleben *et al.*, "Photon flux determination of a liquid-metal jet X-ray source by means of photon scattering," *J. Anal. At. Spectrom.*, vol. 34, no. 7, pp. 1497–1502, 2019. doi: 10.1039/C9JA00127A
- [2] V. Hauk, *Structural and Residual Stress Analysis by Nondestructive Methods: Evaluation - Application - Assessment*. Amsterdam: Elsevier Science, 1997.
- [3] E. Macherauch and P. Müller, "Das sin²psi-Verfahren der röntgenographischen Spannungsmessung," *Z. Angew. Phys.*, vol. 13, pp. 305–312, 1961.
- [4] H. Ruppertsberg, I. Detemple, and J. Krier, "Evaluation of strongly non-linear surface-stress fields $\sigma_{xx}(z)$ and $\sigma_{yy}(z)$ from diffraction experiments," *Phys. Status Solidi*, vol. 116, no. 2, pp. 681–687, Dec. 1989. doi:10.1002/PSSA.2211160226
- [5] C. Genzel, "Formalism for the evaluation of strongly non-linear surface stress fields by X-ray diffraction performed in the scattering vector mode," *Phys. Status Solidi*, vol. 146, no. 2, pp. 629–637, Dec. 1994. doi:10.1002/PSSA.2211460208
- [6] C. Genzel, I. A. Denks, J. Gibmeier, M. Klaus, and G. Wagener, "The materials science synchrotron beamline EDDI for energy-dispersive diffraction analysis," *Nucl. Instrum. Methods Phys. Res., Sect. A.*, vol. 578, no. 1, pp. 23–33, Jul. 2007. doi:10.1016/j.nima.2007.05.209
- [7] M. Klaus and F. Garcia-Moreno, "The 7T-MPW-EDDI beamline at BESSY II," *J. Large-scale Res. Facil. JLSRF*, vol. 2, Jan. 2016. doi:10.17815/jlsrf-2-63
- [8] C. Genzel, M. Meixner, D. Apel, M. Boin, and M. Klaus, "Nondestructive residual stress depth profile analysis at the inner surface of small boreholes using energy-dispersive diffraction under laboratory conditions," *J. Appl. Crystallogr.*, vol. 54, no. 1, pp. 32–41, Feb. 2021. doi:10.1107/S1600576720014508
- [9] H. Näsström *et al.*, "Dependence of phase transitions on halide ratio in inorganic CsPb(Br x I 1-x) 3 perovskite thin films obtained from high-throughput experimentation," *J. Mater. Chem. A*, vol. 8, no. 43, pp. 22626–22631, 2020. doi:10.1039/D0TA08067E
- [10] F. García-Moreno, P. H. Kamm, T. R. Neu, and J. Banhart, "Time-resolved in situ tomography for the analysis of evolving metal-foam granulates," *J. Synchrotron Radiat.*, vol. 25, no. 5. Wiley-Blackwell, pp. 1505–1508, Sep. 01, 2018. doi:10.1107/S1600577518008949
- [11] F. García-Moreno *et al.*, "Using X-ray tomography to explore the dynamics of foaming metal," *Nat. Commun.*, vol. 10, no. 1, p. 3762, Dec. 2019. doi:10.1038/s41467-019-11521-1
- [12] F. García-Moreno *et al.*, "Tomography: Time-Resolved Tomography for Dynamic Processes in Materials," *Adv. Mater.*, vol. 33, no. 45, p. 2104659, Nov. 2021. doi:10.1002/ADMA.202104659
- [13] C. Jiménez *et al.*, "Possibilities for In-Situ Imaging of Metallic and Polymeric Foams using Laboratory Liquid Metal Jet and Microfocus X-Ray Sources," in *Metfoam, 9th Int. Conf. on Porous Metals and Metallic Foams*, 2015. doi:10.13140/RG.2.1.3563.9281
- [14] C. Jiménez *et al.*, "Simultaneous X-ray radiography/tomography and energy-dispersive diffraction applied to liquid aluminium alloy foams," *J. Synchrotron Radiat.*, vol. 25, no. 6, pp. 1790–1796, Nov. 2018. doi:10.1107/S1600577518011657